Progress in Eigenvalue Elasticity Analysis as a Coherent Loop Dominance Analysis Tool

Burak Güneralp

University of Illinois at Urbana-Champaign
Department of Natural Resources and Environmental Sciences
S. Goodwin Ave. Urbana IL 61801 USA
Telephone: ++1 217 333 93 49
Fax: ++1 217 244-3219
guneralp@uiuc.edu

Abstract

Formal model analysis tools are essential elements in understanding how structure drives behavior. Conventional model analysis relies heavily on a time-consuming experimental iterative process. Current formal tools are not mature enough for application to most models. This paper presents a loop dominance analysis approach based on eigenvalue elasticity analysis. Eigenvalue elasticity analysis, although a potentially strong formal model analysis tool, has drawn criticisms over the years for a number of reasons. The approach proposed in this study attempts to bring proper solutions to the issues raised by those criticisms. To this end, a ten-step procedure is proposed. Among the most prominent features of the proposed procedure is the ability to track the influences of feedback loops on a specific variable of interest. Others include the ability to track the loop dominance dynamics over time and an attempt to the codification of the proposed features of the eigenvalue elasticity analysis. Several programming codes, written for this purpose in mind, are presented in the paper. The application of the proposed approach is demonstrated using a simple economic long wave model and two other models, all chosen from earlier methodological studies on formal loop dominance analysis. The results of these applications also facilitate the comparison of the proposed approach to other formal model analysis tools.

Keywords: Loop dominance, nonlinear dynamics, complex systems, eigenvalue elasticity analysis, formal model analysis, model structure, economic long wave.

1. Background

1.1. Motivation

The concept of feedback in systems thinking essentially stems from the notion that endogenous sources are responsible for the creation of system behavior. Akin to this view, the premise of the system dynamics has been to bring understanding to how structure drives behavior. "Understanding model behavior" has claimed the first rank in a list of eight problem areas put forward as currently deserving the attention of system dynamics practitioners (Richardson 1996).

Although the importance of structure in unfolding of model behavior is acknowledged, the formal tools to reveal how structure generates behavior have largely been missing in the system dynamics applications. The established practice in model analysis in system dynamics field is to formulate relevant hypotheses and to perform repeated simulations to test them. Furthermore, this experimental approach has to be coupled with intuition and experience on the part of the analyst in order the approach to be fruitful. The difficulty of carrying out this process becomes burdensome even for experienced modeler in dealing with complex models. While this approach is a necessary part of model analysis and probably will never be completely replaced it should be supported by formal analysis tools in order to increase the efficacy of the

existing practice. Over the years, there have been attempts towards a better understanding of structure-behavior linkages and the formulation of formal tools for this purpose (Forrester 1982; Davidsen 1991; Richardson 1995; Ford 1999; Saleh 2002; Mojtahedzadeh *et al.* 2004; Oliva 2004).

The earliest and mathematically the most rigorous of the formal model analysis tools is the eigenvalue elasticity analysis (Forrester 1982). This study is an attempt to advance the eigenvalue elasticity analysis as a methodology for tracking the dynamics of feedback loop dominance in high-order nonlinear models. The overall goal is to develop a theoretical and methodological framework to uncover structure-behavior relationships in highly complex nonlinear models. Specific objectives of the research are to determine the dominant behavior modes in highly nonlinear models and the contribution of models' feedback loops to these dominant modes.

The research holds promise of opening ways for possible theoretical developments in how certain feedback loops operate together to give rise to various behavior modes in nonlinear models (Güneralp 2004). Practical contributions will be identification of parameters that play a significant role in generating the dynamics of a model. This improvement would lead to identification of efficient policy leverage points in the particular system under study. Finally, successful implementation of the proposed methodology on a model would increase the credibility of the model for use in policy analysis and decision-making practices. Accomplishment of these objectives will contribute to the analysis of complex nonlinear systems by providing a numerical tool to identify significant causal structures that underlie the dominant behavior modes in highly nonlinear systems.

This paper presents the results of the first stage of the research on loop dominance dynamics. The later stages of the research will concentrate on the coupling of the eigenvalue elasticity analysis with the error analysis tools (Gertner 1987). Important objectives of this type of analysis include the identification and quantification of different sources of uncertainty that propagate through the model affecting model behavior patterns. The coupling will enable to identify the effects of parameter uncertainty on the loop dominance dynamics in a model. The broader impact of the research when completed will be twofold: Its contribution to the analysis of complex systems by bringing a new understanding to how structure drives behavior in nonlinear models, and by identifying the effect of parameter uncertainty on these structure-behavior relations.

1.2. Loop dominance analysis

Analyzing the structure-behavior relationship in a model essentially reveals what parts (which feedback structures) are responsible for which behavior mode of the model and to what extent. The central theme in uncovering structure-behavior relations is the "dominant loop" concept. The model behavior evolves as a consequence of the dynamic interactions between various feedback loops of the model. As a result, the influence of any feedback loop at any time on the generation of model behavior may change. The most influential structure in determining some segment of the dynamics of a system is called dominant and the analysis that aims to uncover these loops is called the loop dominance analysis.

Uncovering dominant feedback structures is important in a number of ways. For instance, they may assist in formulating principles on how certain feedback loop combinations function in concert to generate observed behavior patterns. Graham (1977) constitutes the first and only attempt in organizing a set of such principles. Recently, Güneralp (2004) presented interesting results on the structure-behavior relationships on a set of linear models that may also have potential implications for nonlinear systems.

Loop dominance analysis has attracted the attention of a handful of system dynamics researchers. These studies approached the subject from different points of view. On the one hand, there are structure-oriented

tools such as eigenvalue elasticity analysis (EEA) and pathway participation metrics (PPM). On the other, there is the behavior-oriented approach of Ford (1999).

Forrester (1982) is the first to lay out the foundations of the eigenvalue elasticity analysis in the system dynamics field. The practice consists of linearizing the model under study at any point in time, calculating its eigenvalues and then noting how the eigenvalues change as causal link gains change in the linearized model. The eigenvalues can be thought of as different behavior modes the superposition of which gives rise to the observed behavior of the system. Thus, EEA, by forming a connection between the model structure and behavior, provides a means to figure out the dominant structure in the model.

The EEA approach requires identifying all feedback loops and all links they pass through in the model. If the model is highly complex with tens of feedback loops this procedure becomes prohibitively difficult. To alleviate the problem, first Kampmann (1996) then Oliva (2004) came up with techniques that allow for using a relatively small number of loops to determine the most influential structure in the model.

The rigor in the mathematical foundations of the EEA also seems to be one of its disadvantages. The approach is repeatedly criticized over its reliance on abstract mathematical constructs such as eigenvalues, which make little sense to the less mathematically advanced. Another weakness of the approach is that it is conventionally used to identify dominance at the level of the model. In other words, it fails to relate the identified dominant structure to any selected variable of interest (Ford 1999).

The most recent contribution to the loop dominance analysis has come from Saleh (2002). Saleh, besides introducing a new measure, called *behavior pattern index* to quantify the behavior pattern of a state variable, refined many aspects of the eigenvalue analysis including its application to nonlinear models. His study once more showed that the EEA is perfectly suited for application to nonlinear models.

A model at its outset may contain a number of redundant substructures. The dominant behavior mode(s) of the system under study could also be captured without these substructures. Hence, eigenvalue analysis can also be used to simplify linear models by retaining selected behavior modes (Eberlein 1984).

Mojtahedzadeh (1997) has proposed another mathematical tool that would aid in understanding structure-behavior linkages. His method makes use of a pathway participation metric (PPM), a measure devised based on ideas first elaborated in Richardson (1995). In contrast to the EEA, which traditionally approaches the structure-behavior relations at the level of model, PPM adopts a minimalist approach in that pathways between two state variables are considered as the primary building blocks of influential structure. Eventually, some combinations of pathways define the most influential system structure, which contains a single feedback loop, in determining the behavior of a state variable at a given time interval. PPM stands as the only approach whose features are implemented in an experimental piece of software, *Digest* (Mojtahedzadeh *et al.* 2004).

One criticism directed towards the PPM method is that it identifies only a single feedback loop at any instant to explain the behavior of a selected variable (Saleh 2002). However, there are actually many interacting feedback loops that are influential in generating the behavior of the selected variable at any time interval.

Another problem about the PPM method is its somewhat myopic approach to structure-behavior relationship. In other words, by confining itself to a single path of dominance, the method misses what is going on in the rest of the model and does not capture the model-wide dynamics. It is also possible that as will be discussed later in the paper, PPM approach, in its current form, fails to properly reveal the causes of oscillatory behavior.

Approaching the loop dominance question from the behavioral perspective, the distinguishing feature of Ford's approach is its exclusive emphasis on behavior patterns rather than the structure or system conditions in models (Ford 1999). The behavioral approach defines dominance with three basic behavior modes: linear, exponential and logarithmic. Furthermore, it identifies simultaneous dominance by bringing in the concepts of multiple dominance and shadow feedback structures. While suffering from the similar shortcomings such as the lack of automation and rigor to be applied to large scale complex models the behavioral approach, by adopting a different vantage point and by raising important questions regarding the purpose and implementation of feedback loop analysis, offers new prospects to enhance the potential of existing loop dominance analysis tools.

2. The methodology

Eigenvalue elasticity analysis was first proposed by Forrester (1982) as a method for relating the strengths (gains) of individual feedback loops to the behavior modes of a linear system. Forrester concentrates on the gains of the causal links that constitute the structure of the model. The causal structure of a linear model can be represented as a gain matrix (Eq. 1). Each entry in the gain matrix, which is equivalent to the Jacobian used in linear analysis near an equilibrium point, represents a compact net gain that represents the slope of the relationship between the net rate of the state variable p and the state variable q, i.e. the change in the net rate of the state variable p in response to a change in the level of the state variable q, $\partial \dot{x}_p / \partial x_q$.

Each eigenvalue of the gain matrix **G** represents an elemental behavior mode the system is capable of generating. These elemental behavior modes (or behavior mode, in short) that may be present in a model are:

(a) Monotonic convergent behavior mode associated with a real negative eigenvalue;
(b) Monotonic divergent behavior mode associated with a real positive eigenvalue;
(c) Sustained oscillatory behavior mode associated with a complex conjugate pair of eigenvalues with zero real parts;
(d) Convergent oscillatory behavior mode associated with a complex conjugate pair of eigenvalues with negative real parts; and
(e) Divergent oscillatory behavior mode associated with a complex conjugate pair of eigenvalues with positive real parts.

These five behavior modes are shown in Figure 1 in the order they are listed. For monotonic convergent behavior mode, the eigenvalue represents its decay rate, the reciprocal of which is the characteristic time constant τ of the behavior mode. Similarly, a negative real part of a complex eigenvalue pair determines the decay rate of an exponential envelope around the oscillations. If the real part of a complex eigenvalue pair is positive the oscillations will grow with time. On the other hand, the imaginary part of a complex eigenvalue pair determines the observed frequency of the oscillations (Franklin *et al.* 2002).

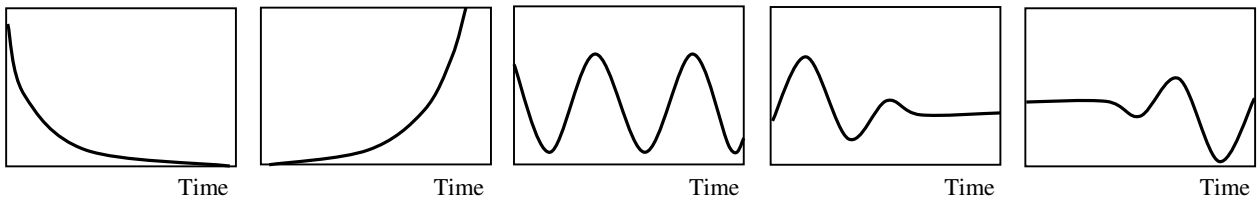

Figure 1. Five behavior modes of Eigenvalue Elasticity Analysis.

The superposition of these behavior modes gives rise to the observed behavior patterns of the model variables. The gains are combinations of the model variables. Therefore, a change in the value of a certain variable changes values of certain gains and thus modifies the behavior modes of the model (i.e. changes the eigenvalues of the model). This may result in an alteration of the overall model behavior. Thus, in the EEA, eigenvalues and eigenvectors characterize the global link between the model structure and behavior.

$$\mathbf{G} = \begin{bmatrix} \partial \dot{x}_1 / \partial x_1 & \cdots & \partial \dot{x}_1 / \partial x_n \\ \vdots & \ddots & \vdots \\ \partial \dot{x}_n / \partial x_1 & \cdots & \partial \dot{x}_n / \partial x_n \end{bmatrix} \tag{1}$$

The EEA can be used for formal model analysis even when the system under study is highly nonlinear (Kampmann 1996, Saleh 2002). The gain matrix of a nonlinear model can be imagined as one the entries of which change over the simulation time due to nonlinear interactions between its elements. However, at sufficiently small time intervals such as the simulation time step, the entries of the gain matrix of a nonlinear model can be assumed to be constants. In other words, the dynamics of the original model is approximated through time by the behaviors of a series of linear models with varying entries in their gain matrices. Then the EEA can be applied to these series of gain matrices over simulation time.

Eigenvalue elasticity is a convenient measure of transient-response sensitivity of the model to parameter changes. The elasticity values are dimensionless, so they are comparable with each other. The elasticity of a complex conjugate eigenvalue pair is also a complex conjugate pair. In such a case, the real part of the elasticity gives the effect on the exponential envelope around oscillations, while the imaginary part gives the effect on the empirical frequency of oscillations (Saleh 2002). The magnitude of the elasticity gives the overall sensitivity of the cyclic mode. In particular, causal links with large elasticities are important. If a small number of links have distinctly larger magnitudes than others, this indicates that they define a dominant subset of the model structure. Most of the time, these distinct links happen to form feedback loops in the model. A detailed explanation on the computation of eigenvalue elasticities is provided in Appendix A.1.

A complete description of link elasticities allows one to calculate loop elasticities. This idea is based on a property of elasticity that the sum of all link elasticities arriving at a node, that is a variable in the model, equals the sum of all link elasticities departing that node. This allows one to set up a system of simultaneous linear equations the solution of which identifies the loop elasticities of the model (Forrester 1983, Kampmann 1996). In general, the magnitude of elasticity measures the overall importance of a loop to a behavior mode. The magnitude can be used to rank loops according to their dominance over each mode.

The implementation of this procedure to calculate loop elasticities becomes unreasonably difficult if the model consists of many feedback loops. Kampmann (1996) discovered that a small subset of loops is sufficient to explain the most influential substructure of a system dynamics model. However, the "independent loop set" obtained is not unique in most instances and making matters worse, the resulting structure-behavior explanations depend on the particular independent loop set. Recently, Oliva (2004) came up with an improvement over the "independent loop set" concept where he, drawing upon the graph and network theory concepts, proposes an algorithm to put feedback loops of a model in a hierarchical order. The algorithm produces a "shortest independent loop set (SILS)". The number of loops identified this way and their length is unique. Although the SILS is not unique the SILS algorithm does generate a

unique outcome from a given model structure. The SILS algorithm resolves the problem of arbitrarily forming *an* independent loop set. It also eliminates the need for using somewhat complicated approaches such as Mason's rule and solving the characteristic equation to directly calculate loop elasticities as proposed by Gonçalves *et al.* (2000). Although the system of equations will still be overdetermined for a typical-sized system dynamics model, it will be consistent and hence will yield a unique solution in terms of loop elasticities (Kampmann 1996).

Oliva and Mojtahedzadeh (2004) has shown on a simple economic long wave model that the most influential loops determined by the PPM method are contained in the SILS of the model. Therefore, it is possible to explain the core dynamics based on the loops selected using the SILS method. However, as they mentioned in their paper, coupling SILS with the EEA would allow for an exploration of interacting feedback loops based on the simplest, most granular and intuitive loops. Therefore, the resulting analysis will be system-wide rather than local and based on an intuitive set of loops. This paper presents, among other examples, the results of and a discussion on a joint implementation of SILS and the EEA on a simple long wave model.

As with every other loop dominance analysis tool, the EEA is still in its formative phase and because of this, criticisms over its implementation have not been missing in the literature (Ford 1999, Mojtahedzadeh *et al.* 2004). The problems these criticisms raise and how they are tackled in this study are explained in the following paragraphs. It is hoped that the proposed approach will advance the EEA as a methodology for tracking the dynamics of feedback loop dominance in highly nonlinear models.

First, a typical application of the EEA amounts to a loop dominance analysis at the level of the model under study. In other words, while behavior modes and the most influential parts of the model are identified one could not be able to explicitly relate these findings to any state variable in the model. Saleh showed that it is possible to break the relative changes in net rate of any state variable at any time down to its constituents each of which is due to each behavior mode of the system. In this paper, it is shown that by further elaboration, the contribution of each behavior mode on any selected state variable can be quantified at any time over the simulation run. The following is a brief explanation of the approach; the details are presented in Appendix A.

During simulation, the dominance of each behavior mode may change over time as a result of the dynamics among various feedback loops of the system. These changes in turn are reflected in the overall behavior pattern of the system. As mentioned above, the model behavior is a linear combination of all behavior modes represented by the eigenvalues of the system (Eq. 2). Thus the contributions of behavior modes on the overall behavior at any instant can be examined independently as follows.

$$\mathbf{s} = \alpha_1 \mathbf{r}_1 + .. + \alpha_i \mathbf{r}_i + .. + \alpha_n \mathbf{r}_n \tag{2}$$

where $\mathbf{s}$ is the slope vector, $\mathbf{r}_i$ is the right eigenvector associated with the i^{th} behavior mode, and α_i is the coefficient of the i^{th} behavior mode, given by

$$\alpha_i = \alpha_i^0 e^{\lambda_i (t - t_o)} \qquad i = 1...n \tag{3}$$

where t_o is the initial time, α_i^0 are the initial values of α_i at t_o and λ_i is the eigenvalue representing the i^{th} behavior mode.

$$s_{ip}{}^{0} = \alpha_i^0 e^{\lambda_i (t_o - t_o)} r_{ip} = \alpha_i^0 r_{ip} \tag{4}$$

$$s_{ip}{}^{dt} = \alpha_i^0 e^{\lambda_i (dt - t_o)} r_{ip} \tag{5}$$

At each time step interval, Eq. 4(5) gives the portion of initial (final) slope of the state variable of interest p coming from the i^{th} behavior mode. The change in the state variable p due to the i^{th} behavior mode is then

$$\Delta s_{ip} = s_{ip}^{\ dt} - s_{ip}^{\ 0} \tag{6}$$

The resulting changes in overall behavior reveal the contribution of each behavior mode on the state variable of interest. The comparison between the contributions of behavior modes becomes easier when the changes they induce are normalized by the sum of the absolute values of those changes. Then the ratio of the change due to that behavior mode and the sum of absolute changes gives the relative contribution of each behavior mode to the overall behavior of the variable of interest (Eq. 7). The rescaled changes vary between –1 and 1. A negative rescaled change at any time step means that behavior mode decreases the slope of the state variable of interest in that interval. A positive change, however, means that the behavior mode increases the slope of the state variable of interest in that interval. The closer the rescaled change is to –1 or 1, the greater the change in the slope due to that behavior mode. It is worth mentioning that the rescaled contribution values tell nothing about the nature of the behavior mode it belongs or that of the overall behavior pattern.

$$c_{ip} = \frac{\Delta s_{ip}}{\sum_{m=1,\,p}^{\mathrm{n}} \left|\Delta s_{mp}\right|} \qquad i = 1...\mathrm{n} \tag{7}$$

Second, there is the question of how dominant behavior modes play out throughout the simulation. It is possible that not every state variable of a model exhibits the same behavior mode. As mentioned in the previous paragraph, the specification of a variable of interest also addresses the issue of different variables simultaneously exhibiting different behavior patterns.

Third, it is also possible that the behavior mode exhibited by any state variable be composed only of a single dominant behavior mode at all times during the simulation. There may be brief periods where the dominant behavior mode of a state variable changes from one behavior mode to another or even periods of considerable length during which more than one behavior mode dictates the behavior mode of one or more state variable. These situations certainly have implications on determining the dominant feedback structure. The conventional approach in EEA is to pick up a single behavior mode as the dominant one, look at which loop(s) it is most sensitive to and then claim them (those) as the dominant substructure. This approach, however, simply fails when there is more than a single dominant behavior mode to explain the behavior of the selected variable. Nevertheless, the quantification of the contribution of each behavior mode to the behavior exhibited by the selected state variable offers a way out. The rescaled contribution values of behavior mode may serve as weights for those behavior modes (Eq. 7). This way one can say, for example, that 60 percent of change in the state variable of interest is due to behavior mode *a* while the remaining 40 percent is due to behavior mode *b* at a particular time step. These values can be used as weights for the loop elasticities of each behavior mode for each loop in the "shortest independent loop set". The resulting values would then reflect the overall influence of loops over the behavior of the state variable of interest at any time step:

$$oe_k = \sum_{i=1}^{\mathrm{n}} c_i e_k^i \qquad k = 1..\mathrm{K} \tag{8}$$

where e_k^i is the elasticity of i^{th} behavior mode to loop k.

Since what we really care about is the relative importance of the feedback loops in creating the system dynamics it would be better if the overall loop elasticities obtained through Eq. 8 are normalized by the sum of their absolute values (Eq. 9). The rescaled overall loop elasticities vary between –1 and 1. A negative loop elasticity at any time step means that that loop drives the behavior of the state variable of interest overall in that interval in negative direction. A positive elasticity, however, means that the loop drives the behavior overall in positive direction. The closer the overall loop elasticity is to –1 or 1, the greater the influence of the corresponding loop.

$$re_k = \frac{oe_k}{\sum_{j=1}^{\mathrm{K}} \left| oe_j \right|} \qquad k = 1..\mathrm{K} \tag{9}$$

Fourth is the lack of automation, which remains as a stringent obstacle to widespread implementation not only of EEA but of other loop dominance analysis methods as well (Ford 1999, Saleh 2002). While a necessity, the automation issue is neither something to be resolved in any one study nor in a short period of time. The new tool that is presented in this study for the analysis of the structure-behavior relationship should therefore be seen as a humble attempt towards the full automation of EEA features. Nevertheless, it serves as a starting point for more advanced implementations of the methodology. For this purpose, several pieces of computer code have been written. A piece of code was written in C language whose main function is to provide the communication between the modeling/simulation software Vensim® and MATLAB® where the actual loop dominance analysis is carried out. Vensim® is selected because of its advanced data handling capabilities. Its Monte Carlo sensitivity analysis module will also be used in the later stages of this research. MATLAB®, on the other hand, is a tool for algorithm development, data visualization, data analysis, and numerical computation with matrices and vectors. The pseudo-codes for the codified portions of the analysis are provided along with brief descriptions of their functions in Appendix B.

3. The feedback loop dominance analysis procedure

The proposed methodology is formulated as a ten-step procedure. Apart from reflecting where the EEA currently stands in loop dominance analysis this sequential approach is a step forward towards the establishment of the EEA as a formal loop dominance method. While tools to carry out some of these steps are available in some of the commercial SD software others still require manual labor (e.g. determining the pathways between state variables and the gains of those pathways).

The first four steps stand as exploratory structural analysis because they amount to identifying structural characteristics of the system dynamics model. The remaining six steps perform on the structural layout produced by the previous steps and are computationally intensive.

1. Identify and list all nodes (i.e. all elements except the constants and table functions) including the state variables (i.e. stocks) in the model. At this stage, the state variable of interest for which the feedback loop dominance dynamics is to be analyzed can be selected.
2. Identify and list all causal links (except the ones that involve constants and flow-to-stock links) and pathways in the model. The causal links are the structural building blocks of feedback loops and a link elasticity is the sum of elasticities of all loops which that link is a part of. They need to be identified so that their elasticities will be computed and used in obtaining loop elasticities later on. Pathways are causal structures linking one state variable to itself or another. There may be multiple pathways on which a state variable interacts with itself or other state variables in a model. A pathway

may consist of one or more causal links and a causal link may lie on several pathways. Identification of these pathways allows for relating eigenvalue elasticities computed from the compact gain matrix **G** to the elasticities of causal links.

3. Identify and list the feedback loops in the Shortest Independent Loop Set (SILS) for the model using the structural analysis procedure proposed by Oliva (2004). This procedure is an improvement over Kampmann's independent loop set concept in the sense that it greatly reduces the subjectivity in the selection of loops that form the most granular yet comprehensive representation of the model structure. Interested readers are referred to Oliva (2004) for the details of the SILS procedure.
4. Form the gain matrix, which represents the links between state variables in their most compact form. The pathways linking the state variable pairs can be aggregated into single links. The gains of these composite links are the elements of the gain matrix. In linear models, the equations for these composite gains are fairly simple and the values they attain are constant; in nonlinear models, however, they may get quite complicated and their values change over time. This amounts to writing down the model equations and taking the partial derivatives with respect to each state variable.
5. Simulate the model and read the gain matrix, pathway gains, net flows of state variables over time from Vensim into MATLAB. Vensim has built-in functions that allow for exporting simulation output out to be used by other software. A C code was written which reads data necessary for the analysis from Vensim and transfer to MATLAB where most of the rest of the analysis is performed.
6. Determine the characteristics of all elemental behavior modes of the system and the contribution of each behavior mode to the behavior of the state variable of interest. The identification of behavior modes of the system amounts to the computation of the eigenvalues and eigenvectors of the model at each analysis time step. The contribution of each behavior mode at any time step can be determined by sequentially deactivating all but one of the behavior modes and noting the change in the slope vector of the selected variable between consecutive time steps. After a suitable rescaling so that they take on values between –1 and 1, they serve as the weights of the behavior modes that constitute the overall behavior mode of the selected variable for the concerned time interval. As with the rest of the analysis this is repeated at every time step. See Appendix A.1 for a detailed discussion and Appendix B.2 for the pseudo-code of an algorithm that does the relevant computations for third-order models.
7. Compute the elasticities of behavior modes (eigenvalues) with respect to the compact links in the gain matrix. For a detailed explanation and the corresponding equation, Eq. A.9, see Appendix A.1. The pseudo-code of the algorithm that does these computations is given in Appendix B.3.
8. Compute the eigenvalue elasticities with respect to each causal link selected in Step 2. For a detailed explanation and the corresponding equation, Eq. A.10, see Appendix A.1. The pseudo-code of the relevant algorithm is given in Appendix B.4. The algorithm is modified for the analysis of a simple long wave model.
9. Using the links identified in Step 2 and the loops in SILS, form the directed cycle matrix. Directed cycle matrix is a notion borrowed from the graph theory in mathematics and is used to present the information on which cycles (loops) are formed by which links in matrix form. The rows in a directed cycle matrix are links, and the columns are loops where the element d_{ij} of the matrix is 1 if link i is an element of loop j and 0 otherwise. The loop elasticities are related to the link elasticities through the directed cycle matrix (Appendix A.2). The matrix will most surely be overdetermined for almost any system dynamics model. Nevertheless, its rank will be equal to the number of columns, thus will always have a unique solution (Kampmann 1996).
10. Compute and plot the overall loop elasticity values over time and evaluate the findings. Having determined the loop elasticities in Step 9, the overall loop elasticity of any loop can be computed by multiplying that loop's elasticity for each eigenvalue by the corresponding eigenvalue contribution weight (see Step 6) and rescaling between –1 and 1. The resulting loop elasticity values are plotted over time, which enables visualizing the evolution of loop dominance dynamics acting upon the

selected model variable over time. The pseudo-code of the algorithm that does the computations of this step for the simple long wave example is given in Appendix B.4.

4. Application of the proposed methodology

The application of the proposed methodology is illustrated using three models selected based on the criteria that they should come from earlier methodological loop dominance studies and would give the most insight (which also happened to come from the most recent studies) on the potential of the EEA approach. A system story will be weaved around the findings of each model's analysis. This will result in coherent, dynamically correct explanations of how certain parts of the system structure create observed patterns of the system behavior as advocated by Mojtahedzadeh *et al.* 2004. In addition, comparisons with earlier approaches will be presented. The model variable names are in *italics* in the text. The equations of the models used as examples are given in Appendix C.

Yeast Population model

This is a simple second-order nonlinear model of yeast population dynamics. It is previously used in the loop dominance analysis context by Saleh (2002). The stock-flow diagram is presented in Figure 2. The model provides a classical example of overshoot-then-collapse dynamics.

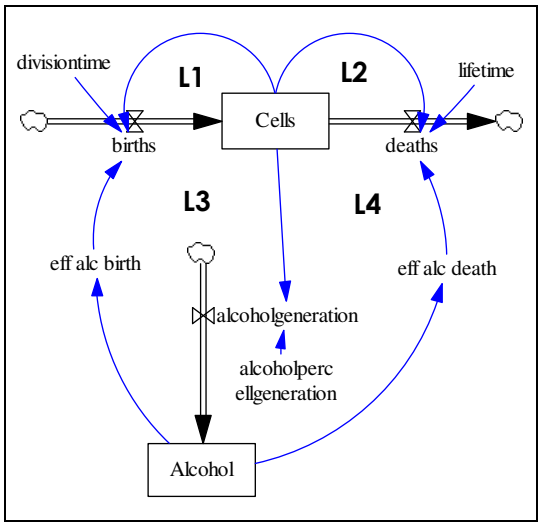

Figure 2. Stock-flow diagram of Yeast model.

1. Identify and list all nodes and choose the state variable of interest.

There are eight nodes in the model: *Cells*, *Alcohol*, *births*, *deaths*, *alcoholgeneration*, *alcoholpercellgeneration*, *eff alc birth*, and *eff alc death*. *Cells* is chosen as the state variable of interest.

2. Identify and list all causal links (except the ones that involve constants and flow-to-stock links) and pathways in the model.

There are seven such causal links in the model and they are listed in Table 1.

Table 1. Causal links of Yeast model relevant to the analysis.

Link no.	Variable sequence
1	Alcohol – eff alc birth
2	Alcohol – eff alc death
3	Cells – alcoholgeneration
4	Cells – births
5	Cells – deaths
6	eff alc birth – births
7	eff alc death – deaths

There are two pathways from *Cells* to itself, one pathway from *Cells* to *Alcohol* and two from *Alcohol* to *Cells* (Table 2).

Table 2. Pathways in Yeast model.

Pathway no.	Variable sequence
1	Cells, births, Cells
2	Cells, deaths, Cells
3	Cells, alcoholgeneration, Alcohol
4	Alcohol, eff alc birth, births, Cells
5	Alcohol, eff alc death, deaths, Cells

3. Identify and list the feedback loops in the Shortest Independent Loop Set (SILS).

The loops in the SILS of Yeast model are listed in Table 3.

Table 3. Feedback loops in the Shortest Independent Loop Set of Yeast model.

Loop no.	Variable sequence
L1	Cells, births
L2	Cells, deaths
L3	Alcohol, eff alc birth, births, Cells, alcoholgeneration
L4	Alcohol, eff alc death, deaths, Cells, alcoholgeneration

4. Form the gain matrix, which represents the links between state variables in their most compact form.

The model is a second-order nonlinear one. Therefore, the dimensions of its gain matrix are 2×2 and the elements of the matrix change continuously over time. The matrix and the partial derivatives are in Eq. 10 and Eq. 11, respectively. The first and second terms in Eq. 11.a are the gains of the Pathways 1 and 2 respectively. Similarly, the first and second terms in Eq. 11.b are the gains of the Pathways 4 and 5 respectively. The partial derivative in Eq. 11.c equals the gain of Pathway 3.

$$\mathbf{G}_{yeast} = \begin{bmatrix} \partial \dot{\text{Cells}} / \partial \text{Cells} & \partial \dot{\text{Cells}} / \partial \text{Alcohol} \\ \partial \dot{\text{Alcohol}} / \partial \text{Cells} & \partial \dot{\text{Alcohol}} / \partial \text{Alcohol} \end{bmatrix} \tag{10}$$

$$\partial \dot{\text{Cells}} / \partial \text{Cells} = \left(\text{eff alc birth} / \text{divisiontime} \right) + \left(\text{-eff alc death} / \text{lifetime} \right) \tag{11.a}$$

$$\partial \dot{\text{Cells}} / \partial \text{Alcohol} = \text{-0.1} * \left(\text{Cells} / \text{divisiontime} \right) + \left(\text{-eff alc death*Cells} / \text{lifetime} \right) \tag{11.b}$$

$$\partial \dot{\text{Alcohol}} / \partial \text{Cells} = \text{alcoholpercellgeneration} \tag{11.c}$$

$$\partial \dot{\text{Alcohol}} / \partial \text{Alcohol} = 0 \tag{11.d}$$

5. Simulate the model and read the gain matrix, pathway gains, net flows of state variables over time.

The behavior of the variable of interest over 90 minutes is shown in Figure 3. The yeast cells grow at a fast rate during the initial phases of the simulation but then as more and more alcohol accumulates in the environment eventually they are wiped out after an even faster decline; thus the overshoot-then-collapse dynamics. The data required to further the analysis is read from Vensim and transferred into MATLAB using the main function whose pseudo-code is in Appendix B.1.

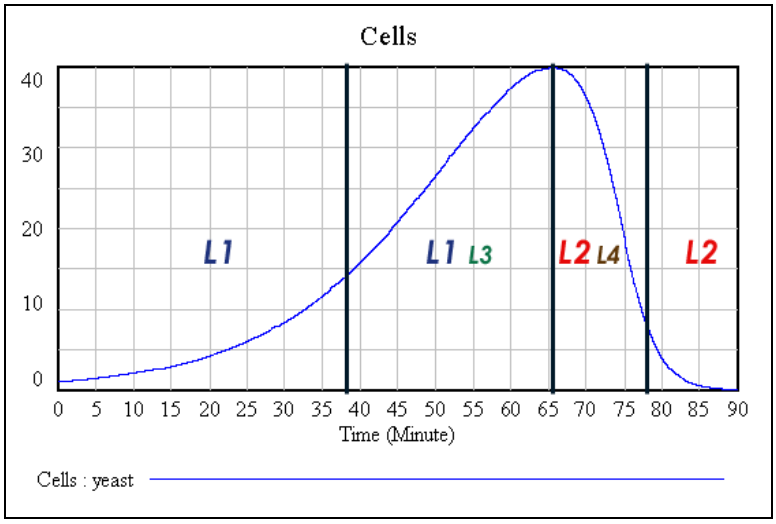

Figure 3. Reference behavior of state variable of interest, *Cells*.

6. Determine the characteristics of all elemental behavior modes of the system and the contribution of each behavior mode to the behavior of the state variable of interest.

The behavior modes that are present at any time step and their relative contributions (weights) to the overall behavior of the variable of interest are provided on Figure 4. The evolution of these behavior modes over time is shown in Figure C.1 of Appendix C.1.

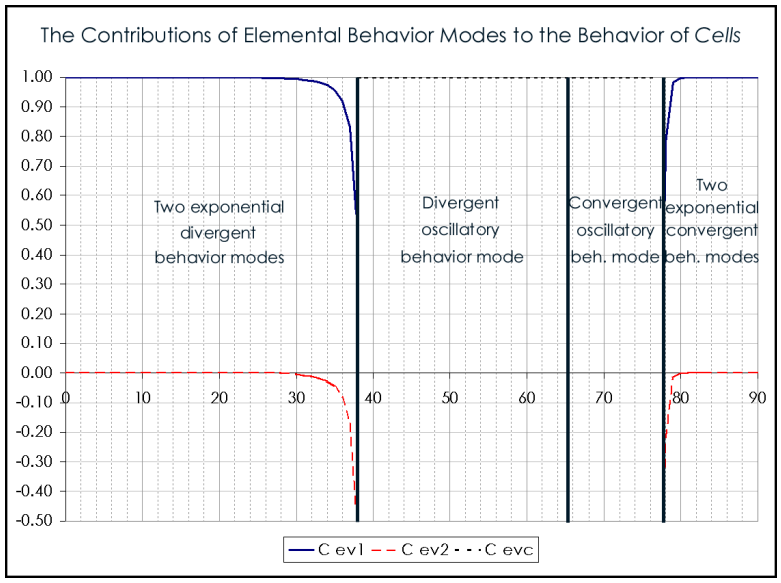

Figure 4. Rescaled contributions of behavior modes on behavior of state variable of interest, *Cells*.

7. Compute the eigenvalue elasticities with respect to compact links in the gain matrix.

The elasticity of each behavior mode is in matrix form as shown in Figure 5. For brevity, the graphs for the elasticities are not shown.

$$\mathrm{E}^{\mathrm{ev1}}_{yeast} = \begin{bmatrix} e^{\mathrm{ev1}}_{11} & e^{\mathrm{ev1}}_{12} \\ e^{\mathrm{ev1}}_{21} & e^{\mathrm{ev1}}_{22} \end{bmatrix} \qquad \mathrm{E}^{\mathrm{ev2}}_{yeast} = \begin{bmatrix} e^{\mathrm{ev2}}_{11} & e^{\mathrm{ev2}}_{12} \\ e^{\mathrm{ev2}}_{21} & e^{\mathrm{ev2}}_{22} \end{bmatrix} \qquad \mathrm{E}^{\mathrm{evc}}_{yeast} = \begin{bmatrix} e^{\mathrm{evc}}_{11} & e^{\mathrm{evc}}_{12} \\ e^{\mathrm{evc}}_{21} & e^{\mathrm{evc}}_{22} \end{bmatrix}$$

(a) (b) (c)

Figure 5. Elasticity matrices for two real eigenvalues (a and b) and complex pair (c).

8. Compute the eigenvalue elasticities with respect to each causal link.

The set of equations that gives the elasticities with respect to each causal link are listed below. For brevity, the graphs for the link elasticities are not shown.

$$e_{cl1} = e_{cl6} = e_{12} * \left(g_{12,pathway4} \Big/ g_{12} \right), \qquad e_{cl2} = e_{cl7} = e_{12} * \left(g_{12,pathway5} \Big/ g_{12} \right)$$

$$e_{cl3} = e_{21}, \qquad e_{cl4} = e_{11} * \left(g_{11,pathway1} \Big/ g_{11} \right), \qquad e_{cl5} = e_{11} * \left(g_{11,pathway2} \Big/ g_{11} \right)$$

where g_{pq} is the gain of compact link from state variable q to p, $g_{pq,pathway\ i}$ is the gain of pathway i from state variable q to p, and e_{pq} is the elasticity to compact link from state variable q to p. The superscripts that identify eigenvalues are omitted for clarity.

9. Using the links identified in Step 3 and the loops in SILS form the directed cycle matrix.

The directed cycle matrix for this model is given in Figure 6. It is a 7×4 matrix and its rank equals 4, the number of loops on the SILS.

	L1	***L2***	***L3***	***L4***
cl1	0	0	1	0
cl2	0	0	0	1
cl3	0	0	1	1
cl4	1	0	0	0
cl5	0	1	0	0
cl6	0	0	1	0
cl7	0	0	0	1

Figure 6. Directed cycle matrix of Yeast model.

10. Compute and plot the overall loop elasticity values over time and evaluate the findings.

The overall loop elasticities are computed and resulting loop dominance dynamics are shown in Figure 7.

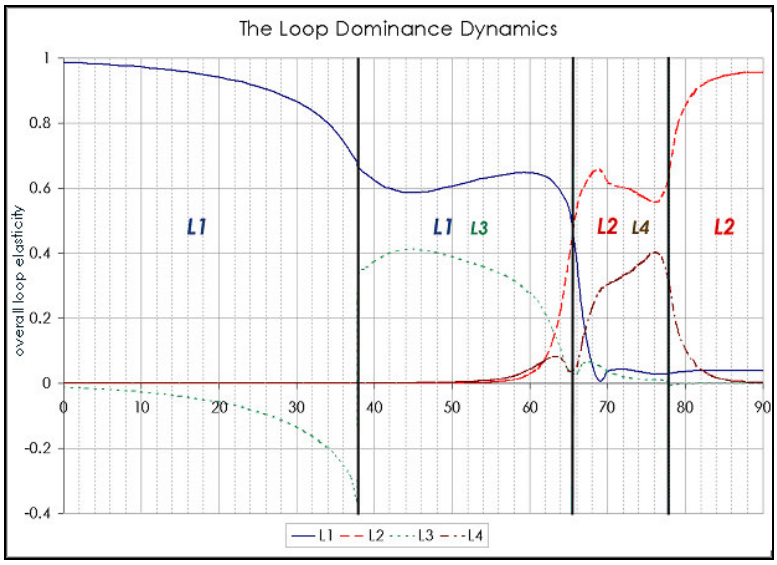

Figure 7. Evolution of loop dominance dynamics for Yeast model over time.

The dynamics that give rise to the well-known overshoot-then-collapse behavior in this particular case is beautifully revealed by the loop dominance analysis. One important distinction of this analysis from the one presented in Saleh (2002) is that the analysis in the latter study was done for only four time steps. Each of these time steps is picked arbitrarily from each period during which different behavior modes are dominant (Figure 4). In contrast, the analysis presented above is truly continuous in time.

Nevertheless, the findings of the two study are in agreement except the third analysis time step at $t = 70$ of Saleh (2002)[1]. First of all, both studies identify four phases of model behavior each characterized by distinct behavior modes: Exponential growth, diverging oscillatory, converging oscillatory, and exponential decay behaviors (See Figure 4 and Figure C.1).

As for the loop dominance dynamics the two studies identify the same loops as dominant except the discrepancy mentioned in the previous paragraph. While loop *L1* is dominant during the exponential growth phase loops *L1* and *L3* are co-dominant during the divergent oscillation phase. The important point is that from the rescaled dominance graph it is not possible to differentiate which loop supports the divergent mode. Close examination of elasticities reveals that loop *L1* supports the divergent mode while loop *L3* has a restraining effect. During the second phase, loop *L1* is mainly responsible for the expansion of the envelope (i.e. its elasticity is substantially high only for the real part) while loop *L3* generates the oscillations (i.e. its elasticity is nonzero only for the imaginary part) although not as strong as loop *L1*.

At minute 65.5, the real part becomes negative, oscillatory mode becomes converging and we pass onto the third phase (Figure C.1). The corresponding elasticity values of the loops change sign accordingly. These loops are *L1* and *L2* since loop *L3* and loop *L4* are only responsible for the generation of the cyclic pattern. This makes sense because loop *L3* and loop *L4* are major loops, in other words pathways for the propagation of disturbances from one state variable to another[2]. Until this point, loop *L3* has lost its influence giving way to loop *L4*; loops *L1* and *L2* are of equal importance though now the elasticity of the first is negative, that of the latter is positive. At minute 68.87, gain of loop *L1* becomes negative and hence its elasticity becomes positive but by now loop *L2* has become the most influential loop on the convergence of the exponential envelope. The influence of loop *L4* is also increasing but it is still smaller than that of loop *L2*.

At minute 77.9, the complex conjugate eigenvalue pair bifurcates and two real and negative eigenvalues emerge, hence the fourth phase: the exponential decay. The elasticities of loops *L1* and *L2* are positive for the larger eigenvalue, negative for the smaller. It is the opposite for loops *L3* and *L4*. However, in terms of magnitude loops *L2* and *L4* have the two largest elasticities. Towards the end of the simulation loop *L2* becomes completely dominant while the resistance of loop *L4* gradually dies away.

The application of the proposed methodology in this simple example enabled showing how loop dynamics evolve over time for a second-order nonlinear model. In addition, this allows tracking the continuous change in *relative* influence of loops in SILS. Another improvement is the fact that a variable of interest, that is *Cells*, is specified and the loop dominance analysis is done for that variable. This is important since the EEA is often critiqued for being too general in its conclusions meaning that the resulting dominant loops could not be associated with a particular variable of interest in the model. Last but not the least, using the contributions of behavior modes on the overall behavior of the variable of interest as weights for the loop elasticities for each of these behavior modes is something new and the preliminary results are promising.

An example with nonlinear oscillations (A Predator-Prey model)

This example is another second-order nonlinear system known as Lotka-Volterra model. It is used by Mojtahedzadeh (1997) to illustrate the application of PPM approach on a nonlinear oscillatory model; thus the following analysis not only illustrates the application of the proposed methodology on a model

[1] The discrepancy is apparently caused by a slight computational error in Saleh (2002).

[2] This observation is in line with the one stated in Güneralp (2004): In a second-order oscillatory system with one major and two minor loops, the negative-polarity major loop is only responsible for the imaginary part whereas the minor loops are mainly responsible for the real part and reduce only slightly the frequency of oscillations.

with sustained nonlinear oscillatory dynamics but it also provides an opportunity to compare the two approaches. The stock-flow diagram is presented in Figure 8.

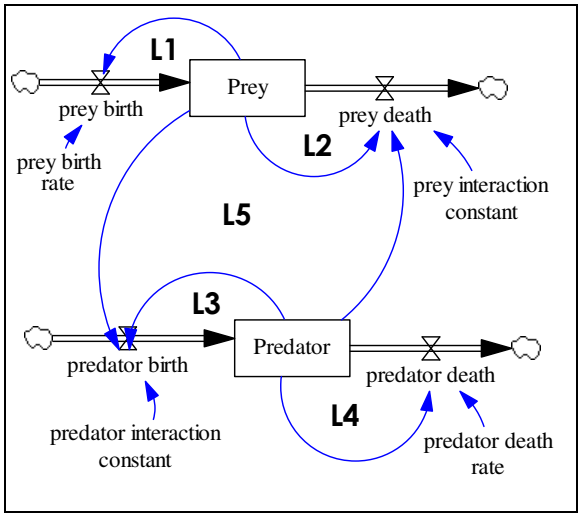

Figure 8. Stock-flow diagram of Predator-Prey model.

1. Identify and list all nodes and choose the state variable of interest.

There are six nodes in the model: *Predator*, *predator birth*, *predator death*, *Prey*, *prey birth*, and *prey death*. *Prey* is chosen as the state variable of interest.

2. Identify and list all causal links (except the ones that involve constants and flow-to-stock links) and pathways in the model.

There are six such causal links in the model and they are given in Table 4.

Table 4. Causal links of Predator-Prey model relevant to the analysis.

Link no.	Variable sequence
1	Prey – prey birth
2	Prey – prey death
3	Prey – predator birth
4	Predator – predator birth
5	Predator – predator death
6	Predator – prey death

There are a total of six pathways: Two pathways from *Prey* to itself, two from *Predator* to itself, one from *Prey* to *Predator* and one from *Predator* to *Prey* (Table5).

Table 5. Pathways in Predator-Prey model.

Pathway no.	Variable sequence
1	Prey, prey birth, Prey
2	Prey, prey death, Prey
3	Predator, predator birth, Predator
4	Predator, predator death, Predator
5	Predator, prey death, Prey
6	Prey, predator birth, Predator

3. Identify and list the feedback loops in the Shortest Independent Loop Set (SILS)[3].

The loops in the SILS of Predator-Prey model are listed in Table 6.

Table 6. Feedback loops in the Shortest Independent Loop Set of Predator-Prey model.

Loop no.	Variable sequence
L1	Prey, prey birth
L2	Prey, prey death
L3	Predator, predator birth
L4	Predator, predator death
L5	Predator, prey death, Prey, predator birth

4. Form the gain matrix, which represents the links between state variables in their most compact form.

The model is a second-order nonlinear one. Therefore, the dimensions of its gain matrix are 2×2 and the elements of the matrix change continuously over time. The matrix and the partial derivatives are shown below:

$$\mathbf{G}_{predator-prey} = \begin{bmatrix} \partial \dot{\text{Prey}} / \partial \text{Prey} & \partial \dot{\text{Prey}} / \partial \text{Predator} \\ \partial \dot{\text{Predator}} / \partial \text{Prey} & \partial \dot{\text{Predator}} / \partial \text{Predator} \end{bmatrix} \tag{13}$$

$$\partial \dot{\text{Prey}} / \partial \text{Prey} = \text{prey birth rate} + \left(\text{-prey interaction constant} * \text{Predator} \right) \tag{14a}$$

[3] For an alternative stock-flow representation of this model, SILS procedure identified only the first four loops leaving out the major loop connecting the two stocks. The alternative representation is given in Figure C.2 of Appendix C.2. Without the major loop the two stocks would be decoupled and there would not be a predator-prey system. This fact and the following analysis illustrate that it is actually an essential loop for the system to oscillate not to mention to exist as it is. Although this is a low-order system it gives sufficient reason to further scrutinize the SILS approach with high-order systems. This example should be regarded as a warning against the faith-based application of the SILS approach –or of any method for that matter.

$$\partial \dot{\text{Prey}} / \partial \text{Predator} = \text{-prey interaction constant} * \text{Prey} \quad (14b)$$

$$\partial \dot{\text{Predator}} / \partial \text{Prey} = \text{predator interaction constant} * \text{Predator} \quad (14c)$$

$$\partial \dot{\text{Predator}} / \partial \text{Predator} = \text{predator interaction constant} * \text{Prey} - \text{predator death rate} \quad (14d)$$

5. Simulate the model and read the gain matrix, pathway gains, net flows of state variables over time.

The behavior of the variable of interest over 60 months is shown in Figure 9. Because the oscillations are sustained, the following analysis is conducted over a period of 30 months, which is approximately the period of oscillations.

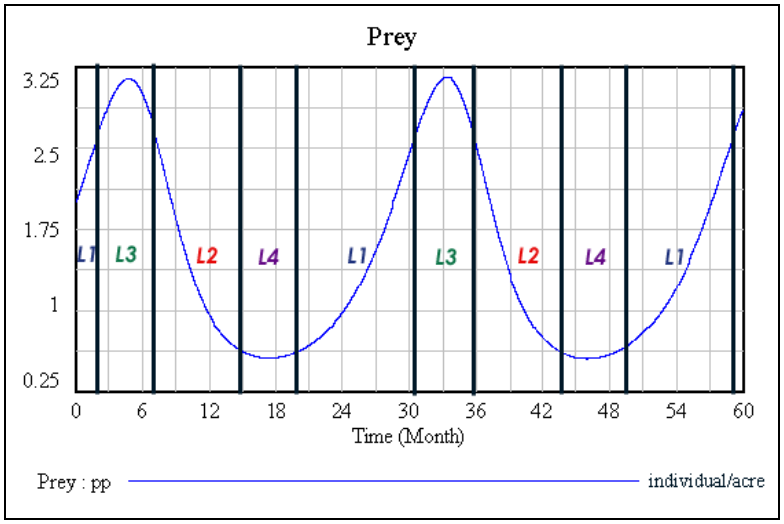

Figure 9. Reference behavior of state variable of interest, *Prey*.

6. Determine the characteristics of all elemental behavior modes of the system and the contribution of each behavior mode to the behavior of the state variable of interest.

The only behavior mode for this model is sustained oscillations, which is reflected in the complex eigenvalue pair of the gain matrix. However, these oscillations are different in nature than the elemental sustained oscillatory behavior mode in the sense that the first are caused by the nonlinear mechanism in the system. Although there is only one complex eigenvalue pair the real and imaginary parts continuously change over time (in fact they oscillate too) because of the nonlinearity in the model. These oscillatory changes in the real and imaginary parts of the eigenvalue pair are the cause of the observed sustained oscillations. Since there is only one complex eigenvalue pair of the model at any time there is no point in calculating the contribution weight, which is obviously one. The figure that shows how the exponential envelope and the frequency of the oscillations (associated with the real and imaginary parts of the complex conjugate eigenvalue pair, respectively) evolve over time, is given in Figure C.3 of Appendix C.2.

7. Compute the eigenvalue elasticities with respect to compact links in the gain matrix.

The elasticity of each behavior mode is in matrix form as shown in Figure 10. For brevity, the graphs for the elasticities are not shown.

$$\mathrm{E}^{\text{ev real}}_{predator-prey} = \begin{bmatrix} e_{11}^{\text{ev real}} & e_{12}^{\text{ev real}} \\ e_{21}^{\text{ev real}} & e_{22}^{\text{ev real}} \end{bmatrix} \quad \mathrm{E}^{\text{ev imag}}_{predator-prey} = \begin{bmatrix} e_{11}^{\text{ev imag}} & e_{12}^{\text{ev imag}} \\ e_{21}^{\text{ev imag}} & e_{22}^{\text{ev imag}} \end{bmatrix}$$

(a) (b)

Figure 10. Elasticity matrices for real (a) and imaginary (b) parts of complex eigenvalue pair.

8. Compute the eigenvalue elasticities with respect to each causal link.

The set of equations that gives the elasticities with respect to each causal link are listed below. For brevity, the graphs for the link elasticities are not shown.

$$e_{cl1} = e_{11} * \left(g_{11,pathway1} \Big/ g_{11} \right), \quad e_{cl2} = e_{11} * \left(g_{11,pathway2} \Big/ g_{11} \right), \quad e_{cl3} = e_{21}$$

$$e_{cl4} = e_{22} * \left(g_{22,pathway3} \Big/ g_{22} \right), \quad e_{cl5} = e_{22} * \left(g_{22,pathway4} \Big/ g_{22} \right), \quad e_{cl6} = e_{12} * \left(g_{12,pathway5} \Big/ g_{12} \right)$$

9. Using the links identified in Step 3 and the loops in SILS form the directed cycle matrix.

The directed cycle matrix for this model is given in Figure 11. It is a 6×5 matrix and its rank equals 5, the number of loops on SILS.

	L1	***L2***	***L3***	***L4***	***L5***
cl1	1	0	0	0	0
cl2	0	1	0	0	0
cl3	0	0	0	0	1
cl4	0	0	1	0	0
cl5	0	0	0	1	0
cl6	0	0	0	0	1

Figure 11. Directed cycle matrix of Predator-Prey model.

10. Compute and plot the overall loop elasticity values over time and evaluate the findings.

The overall loop elasticities are computed and resulting loop dominance dynamics impacting the exponential envelope and the observed frequency of oscillations are shown in Figure 12. The loop dominance dynamics impacting the oscillatory behavior as a whole are shown in Figure 13.

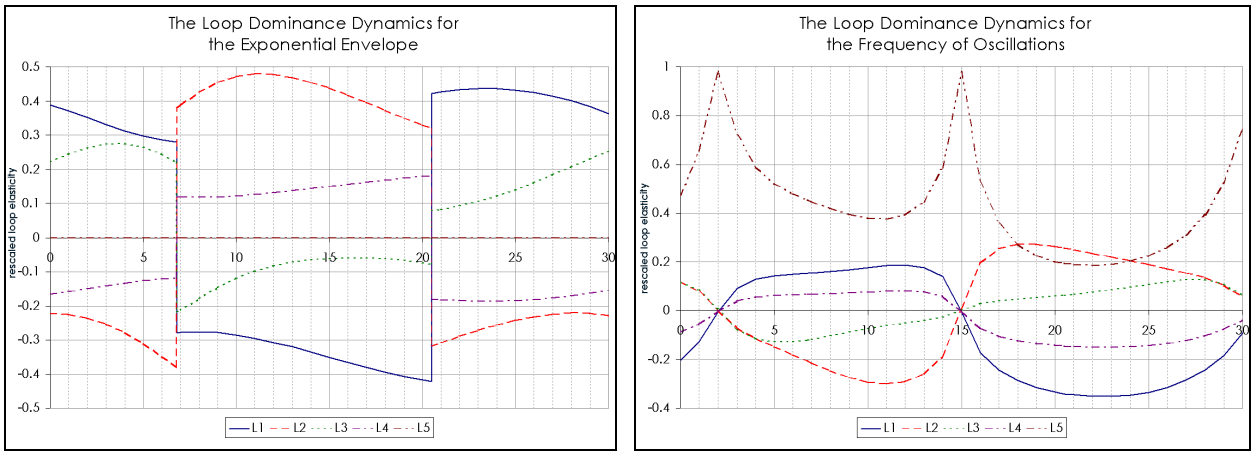

(a) *(b)*

Figure 12. Evolution of loop dominance dynamics for exponential envelope *(a)* and for frequency of oscillations *(b)* of *Prey* behavior over time.

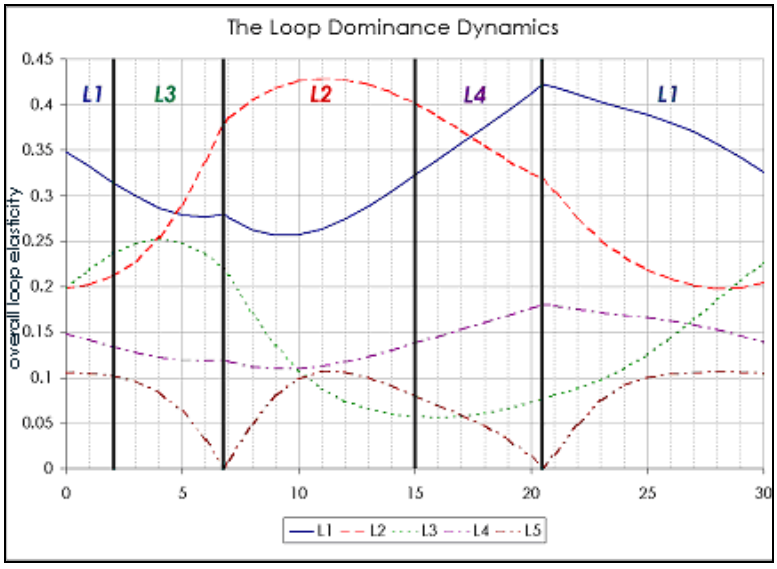

Figure 13. Evolution of loop dominance dynamics for overall behavior of *Prey* over time.

The results of the analysis show how the nature of the sustained oscillations in this nonlinear system differs from the nature of those in linear systems. The oscillations are indeed sustained but this is not because the exponential envelope is non-existent (i.e. real part of the eigenvalue pair is zero) but because the exponential envelope keeps changing due to the nonlinearity in the model (Figure C.3).[4] The exponential envelope is a diverging one during two segments of the period of oscillations. The first of the two segments is between months 0 and approximately 6.80 and the second is between months 20.5 and 30. Between these two segments the exponential envelope is contracting (Figure C.3). Figure 12a shows that both minor birth loops, that is, loops *L1* and *L3* support the diverging exponential envelope but resist when it is in the contracting phase. In contrast, both minor death loops, that is, loops *L2* and *L4* support the contracting envelope but resist when it is in the divergent phase. In addition, it is worth noting that the major loop *L5* plays no role over the exponential envelope.

[4] The nonlinearity is a simple multiplication of the two state variables reflecting the interaction of the two species (See Appendix C.2 for the model equations).

The frequency of oscillations too changes over time (Figure C.3). The major loop *L5* is virtually the only responsible structural piece for the frequency for almost the whole period (Figure 12.b). The elasticities of the prey birth loop *L1* and the predator death loop *L4* are positive (potentially leading to higher frequency of oscillations) for almost half the period and negative (potentially leading to lower frequency) for the rest. The picture is the opposite for the prey death loop *L2* and the predator birth loop *L3*. The minor death loop *L2* is, however, at least as influential as the major loop around month 20 (Figure 12b).

A word of caution in interpreting loop dominance graphs is in order. In Figure 13, although the two minor loops, that is the loops *L1* and *L2*, associated with the state variable *Prey* seems to be the most dominant pair, actually their influences are opposite to each other as revealed in Figure 12a[5]. Because of this and the fact that they act upon the same state variable (i.e. stock), their opposite influences actually cancel out each other when their magnitudes are approximately equal. This is, of course, valid for the minor loops of the state variable *Predator* too. Thus, the actual influence of minor loops on the behavior of variable of interest is in fact revealed by the sum of the influences of minor loops with a common state variable. Accordingly, at any analysis time step, if the sum of the influences of the minor loops of *Prey(Predator)* is larger then the sum of the influences of the minor loops of *Predator(Prey)* then the minor loop of *Prey(Predator)* with the larger magnitude is the dominant loop at that time step. The time segments during each of which a different minor loop of the model is dominant are shown on Figures 9 and 13. Thus the minor prey birth loop *L1*, the minor predator birth loop *L3*, the minor prey death loop *L2* and the minor predator death loop *L4* are each dominant during the fast growth, peaking, slowing decline, and grounding phases, respectively. It is worth noting, though, that the shifts in dominance between these loops are not instantaneous but gradual.

The above explanation is almost totally in agreement with the one based on the PPM analysis (Mojtahedzadeh 1997). The only disagreement may stem from the interpretation of the role of the major loop *L5*. According to the PPM analysis the major loop plays relatively less significant role. The significance of its role is actually high, but it becomes evident only when the influences of each loop on the frequency of oscillations (i.e. the imaginary part of the eigenvalue pair) are plotted (Figure 12b). This fact, however, is not revealed with the PPM approach. It must be emphasized that the oscillations would not occur at all if there were no such loop that connects the two stocks (Figure 12b). The major loop's overall influence is not prominent compared to the minor loops (see Figure 13) but here the situation is certainly not as simple as that by the fact that the minor loops would not function as they do now without the presence of a major loop.

Another difference between the EEA and the PPM approaches is that the first gives a more complete picture in the sense that one is able to trace the *gradual* shifts in loop dominance through simulation and at the same time observe the *relative* influences of each loop on the behavior of variable of interest.

On the other hand, this example also shows that one needs to be careful in interpreting the results of the EEA. The overall loop elasticity of the oscillatory behavior does not give much detail on how model structure generates the behavior (Figure 13). One needs to consider the elasticities of the components of the behavior (i.e. the exponential envelope and the frequency) separately in order to reach a better understanding of the structure-behavior dynamics. Furthermore, the relations of loops with each other also need to be considered. Once again, the formal methods should not be regarded as magical devises that reveal all that needs to be known automatically but as tools that merely help to get a better understanding of the dynamics of systems under study.

[5] Recall that the magnitude of the complex elasticity value gives the overall elasticity of the oscillatory behavior; hence, the non-negative loop elasticities in Figure 13.

A simple model of Economic Long Wave

The proposed methodology is also applied to a simple long wave model (Sterman 1985). The model is chosen for a number of reasons. First it is widely known and therefore serves as a suitable test for the proposed methodology. Second, although it has a relatively simple structure it is capable of generating complicated dynamics because of the nonlinearities. Third, it was recently used in a concurrent application of SILS and PPM approaches (Oliva and Mojtahedzadeh 2004). Therefore, it would be interesting to see how the results of a joint application of SILS and the EEA compare to the findings of that study. Finally, the model is also used by Kampmann (1996) and Ford (1999) to illustrate the applications of their approaches. Thus, the application of the EEA on the long wave will also provide an opportunity to compare the proposed approach with the Ford's behavioral approach. It is assumed that the reader is already familiar with the model. The details of the model and its dynamics can be found in Sterman (1985). The stock-flow diagram is presented in Figure 14.

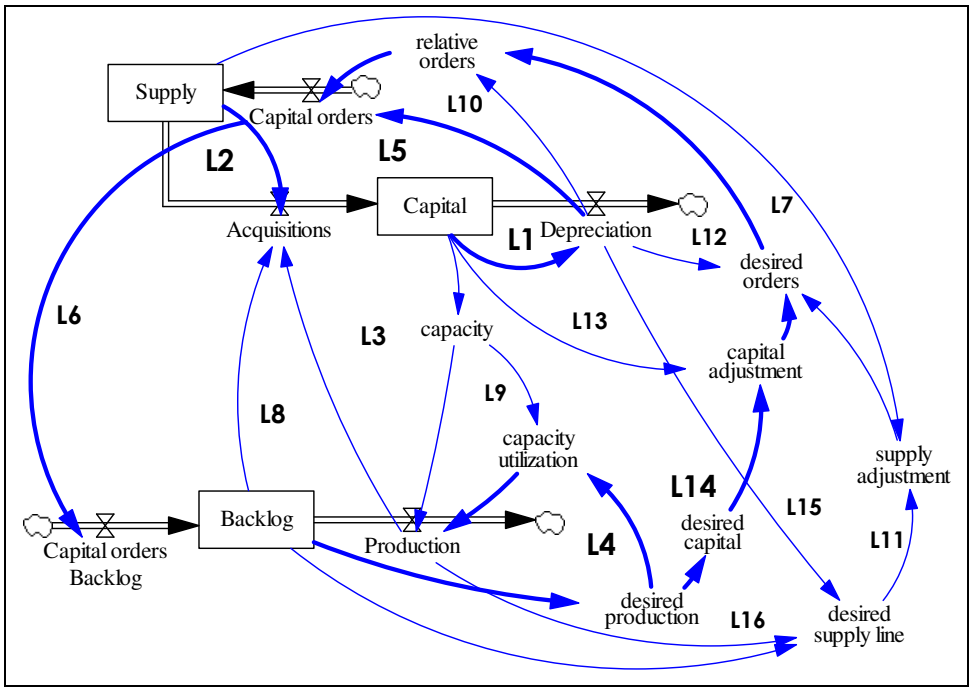

Figure 14. Stock-flow diagram of a simple Long Wave model.

1. Identify and list all nodes and choose the state variable of interest.

There are nineteen nodes in the model. The list of the nodes is in Table C.1 in Appendix C.3. *Capital* is chosen as the state variable of interest.

2. Identify and list all causal links (except the ones that involve constants and flow-to-stock links) and pathways in the model.

There are twenty-six such causal links in the model and they are listed in Figure C.4 in Appendix C.3.

There are thirty-six pathways between the state variables. The pathways originating from *Capital*, *Supply* and *Backlog* are listed in Tables C.2-4, respectively, in Appendix C.3.

3. Identify and list the feedback loops in the Shortest Independent Loop Set (SILS).

There are sixteen loops in the set (Note that 34 {the total number of links} – 19 {total number of nodes} + 1 = 16. See Appendix A.2 for a brief discussion on this relationship). The loops are listed in Table C.5 in Appendix C.3. The loops are also shown on the stock-flow diagram in Figure 14. The numbers of loops that are most influential at one time or another during the simulation are printed with a larger font on the figure. In addition, the corresponding pathways are depicted with thicker lines.

4. Form the gain matrix, which represents the links between state variables in their most compact form.

The model is a third-order nonlinear one. Therefore, the dimensions of its gain matrix are 3×3 and the elements of the matrix change continuously over time. The form of the matrix is shown in Eq. 13. The partial derivative equations are given in Eqs. C.1-9 in Appendix C.3.

$$\mathbf{G}_{longwave} = \begin{bmatrix} \partial \dot{\text{Capital}} / \partial \text{Capital} & \partial \dot{\text{Capital}} / \partial \text{Supply} & \partial \dot{\text{Capital}} / \partial \text{Backlog} \\ \partial \dot{\text{Supply}} / \partial \text{Capital} & \partial \dot{\text{Supply}} / \partial \text{Supply} & \partial \dot{\text{Supply}} / \partial \text{Backlog} \\ \partial \dot{\text{Backlog}} / \partial \text{Capital} & \partial \dot{\text{Backlog}} / \partial \text{Supply} & \partial \dot{\text{Backlog}} / \partial \text{Backlog} \end{bmatrix} \tag{13}$$

5. Simulate the model and read the gain matrix, pathway gains, net flows of state variables over time.

The behavior of the variable of interest *Capital* is sustained oscillations with a period of about 45 years (Figure 15). Therefore, the following analysis is conducted over a period of 46 years from year 136 to 182.

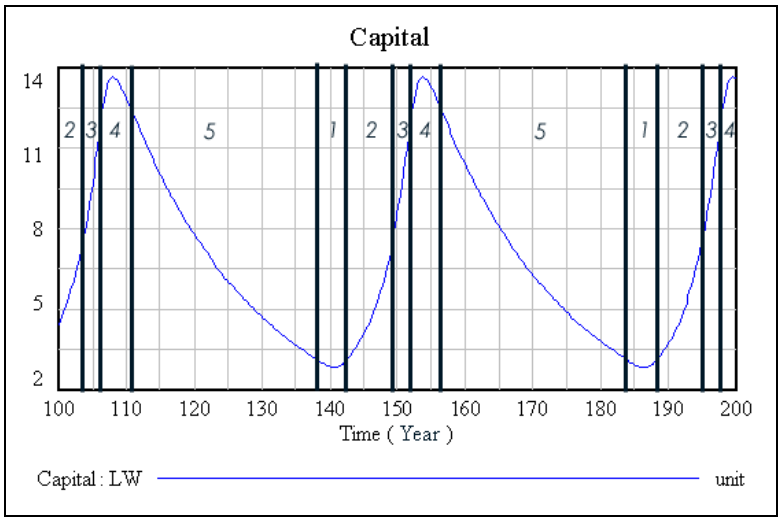

Figure 15. Reference behavior of state variable of interest, *Capital*.

6. Determine the characteristics of all elemental behavior modes of the system and the contribution of each behavior mode to the behavior of the state variable of interest.

Like the Predator-Prey model, the observed behavior for this model is sustained oscillations. However, the oscillations in the long wave are not caused by a single complex conjugate eigenvalue pair. Rather, the oscillatory behavior is composed of various different behavior modes each of which becomes

gradually dominant for certain time segments of the simulation (Figure C.5 and Figure 18.a). There are five distinct segments in a period; hence, the long-wave cycle will be divided into five phases similar to the segmentation of the model behavior in Kampmann (1996).[6] These phases in sequential order are 1."self-order initiation", 2."capital growth", 3."capital deceleration", 4."capital peak-then-decline", and 5."capital depreciation". They are also shown on the behavior of *Capital* on Figure 15.

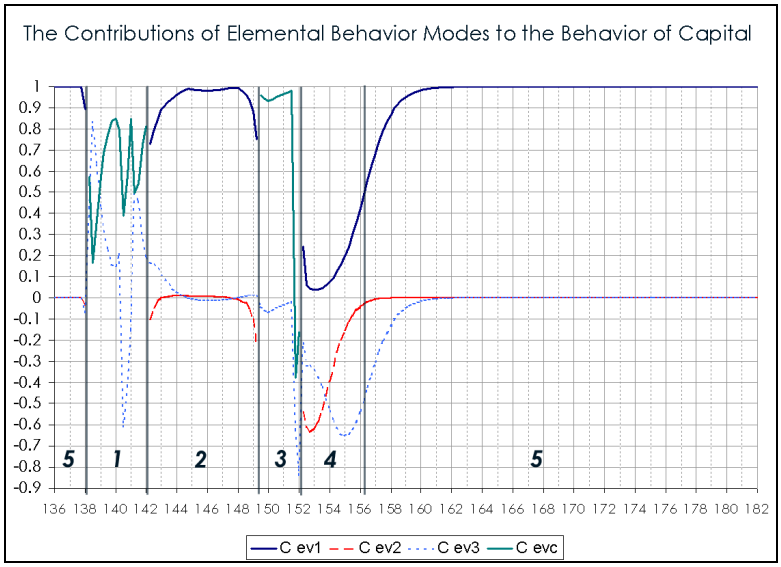

Figure 16. Rescaled contributions of behavior modes on behavior of state variable of interest, *Capital*.

The relative contributions (weights) of the behavior modes that are present at any time step to the overall behavior of the variable of interest are provided on Figure 16. The behavior modes corresponding to each phase are listed in Table 7. The evolution of these behavior modes over time is shown in Figure C.5. Note that there are three convergent behavior modes in the beginning. Two of these modes disappear right after year 138. At the same time, an oscillatory mode, which is initially almost instantaneously converging then for the rest of the phase diverging, emerges (due to the coalescence of the two real positive eigenvalues to give birth to a complex eigenvalue pair) and the "self-order initiation" phase begins. Then oscillatory mode gives way to two behavior modes around year 142 (a consequence of the bifurcation of the complex pair to two real negative eigenvalues) and the "capital growth" phase is initiated. One of these behavior modes is divergent throughout the second phase while the other is convergent for most of the phase except the beginning and ending of the phase. Towards year 150 these two behavior modes disappear. They are replaced by another divergent oscillatory mode, which heralds the beginning of the "capital deceleration" phase. Around year 152, the system enters the "capital peak-then-decline" phase when this oscillatory mode too gives way to two convergent behavior modes. The fourth phase, lasts until about year 157 and the dominant behavior mode is the one with a time constant that varies from about 6 years to 1 year during the phase. However, after a short transitional period the convergent behavior mode with the time constant of about 20 years becomes dominant; hence, the final "capital depreciation" phase.

[6] Kampmann divided the long wave into four segments based on a visual inspection of the model behavior and the changes in eigenvalues. However, calculating the contribution of each eigenvalue in this study reveals that there are actually five distinct phases of the long wave.

Table 7. Behavior modes present in each phase of the long wave.

Phase no.	Phase name	Behavior modes
1	Self-order initiation	One divergent oscillatory, one convergent mode
2	Capital growth	One divergent, two convergent modes
3	Capital deceleration	One divergent oscillatory, one convergent mode
4	Capital peak-then-decline	Three convergent modes
5	Capital depreciation	Three convergent modes

7. Compute the eigenvalue elasticities with respect to compact links in the gain matrix.

The elasticity of each behavior mode is in matrix form as shown in Figure 17. For brevity, the graphs for the elasticities are not shown.

$$\mathrm{E}^{\mathrm{ev1}}_{longwave} = \begin{bmatrix} e^{\mathrm{ev1}}_{11} & e^{\mathrm{ev1}}_{12} & e^{\mathrm{ev1}}_{13} \\ e^{\mathrm{ev1}}_{21} & e^{\mathrm{ev1}}_{22} & e^{\mathrm{ev1}}_{23} \\ e^{\mathrm{ev1}}_{31} & e^{\mathrm{ev1}}_{32} & e^{\mathrm{ev1}}_{33} \end{bmatrix}$$

(a)

$$\mathrm{E}^{\mathrm{ev2}}_{longwave} = \begin{bmatrix} e^{\mathrm{ev2}}_{11} & e^{\mathrm{ev2}}_{12} & e^{\mathrm{ev2}}_{13} \\ e^{\mathrm{ev2}}_{21} & e^{\mathrm{ev2}}_{22} & e^{\mathrm{ev2}}_{23} \\ e^{\mathrm{ev2}}_{31} & e^{\mathrm{ev2}}_{32} & e^{\mathrm{ev2}}_{33} \end{bmatrix}$$

(b)

$$\mathrm{E}^{\mathrm{ev3}}_{longwave} = \begin{bmatrix} e^{\mathrm{ev3}}_{11} & e^{\mathrm{ev3}}_{12} & e^{\mathrm{ev3}}_{13} \\ e^{\mathrm{ev3}}_{21} & e^{\mathrm{ev3}}_{22} & e^{\mathrm{ev3}}_{23} \\ e^{\mathrm{ev3}}_{31} & e^{\mathrm{ev3}}_{32} & e^{\mathrm{ev3}}_{33} \end{bmatrix}$$

(c)

$$\mathrm{E}^{\mathrm{evc}}_{longwave} = \begin{bmatrix} e^{\mathrm{evc}}_{11} & e^{\mathrm{evc}}_{12} & e^{\mathrm{evc}}_{13} \\ e^{\mathrm{evc}}_{21} & e^{\mathrm{evc}}_{22} & e^{\mathrm{evc}}_{23} \\ e^{\mathrm{evc}}_{31} & e^{\mathrm{evc}}_{32} & e^{\mathrm{evc}}_{33} \end{bmatrix}$$

(d)

Figure 17. Elasticity matrices for three real eigenvalues (*a*, *b*, and *c*) and complex pair (*d*).

8. Compute the eigenvalue elasticities with respect to each causal link.

The set of equations that gives the elasticities with respect to each causal link are given in Eqs. C.10-35 in Appendix C.3. For brevity, the graphs for the link elasticities are not shown.

9. Using the links identified in Step 3 and the loops in SILS form the directed cycle matrix.

The directed cycle matrix for this model is given in Figure C.4. It is a 16×26 matrix and its rank equals 16, the number of loops on the SILS.

10. Compute and plot the overall loop elasticity values over time and evaluate the findings.

The overall loop elasticities are computed and resulting loop dominance dynamics impacting the exponential envelope and the observed frequency of oscillations over a whole cycle are shown in Figure 18.a. The loop dominance dynamics over each phase are given in Figures 18.b-f in sequential order.

As the last phase of the previous cycle gives way to the first phase of the next cycle the capacity falls below orders. At this early stage of the self-order initiation phase, the Supply first-order control loop (*L2*) becomes dominant briefly. The reason is that self-ordering mechanism begins to work and increases *Supply* stock. However, acquisitions do not rise fast enough for capacity to catch up with orders and this loop quickly loses its influence; the Capital self-ordering loop (*L14*) becomes the most dominant. After a brief period during which there is no markedly dominant loop the first phase ends (Figure 18.b). The previous analyses identify the importance of the self-ordering loop in this phase but none of them identifies the role played by the Supply first order control loop in the beginning (Kampmann 1996, Ford 1999, Oliva and Mojtahedzadeh 2004).

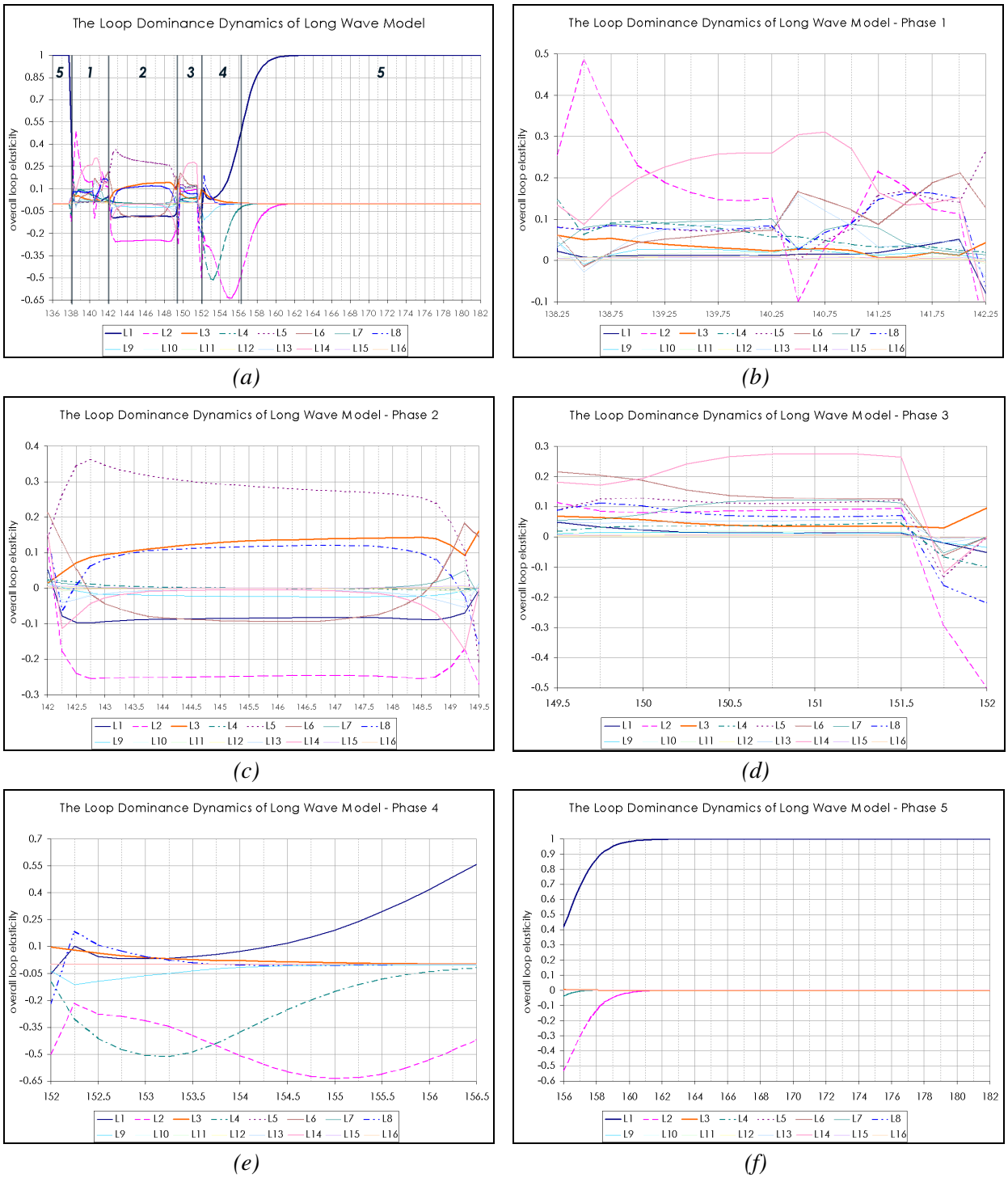

Figure 18. Evolution of loop dominance dynamics for a whole cycle *(a)* and for phase 1 *(b)*, 2 *(c)*, 3 *(d)*, 4 *(e)*, and 5 *(f)* of *Capital* over time.

The capital growth phase is driven by the Capital expansion (*L5*) loop. In addition, the Economic growth (*L3*) and the Order fulfillment (*L8*) loops have relatively large positive elasticities and hence they are also important in creating the behavior of *Capital*. The influences of these loops are countered to a certain extend by the Supply first order control (*L2*), the Capital decay (*L1*), and the Backlog expansion (*L6*)

loops. Nevertheless, their combined effect is not enough to match that of the loops with positive elasticities and *Capital* continues to increase exponentially during this phase. The Capital self-ordering loop, however, becomes completely dormant. In addition, the capacity utilization is at its maximum effectively keeping the first-order Production scheduling (*L4*) loop in check (Figure 18.c). This explanation regarding the importance of the Capital expansion and the economic growth loops agrees with that of Kampmann. However, the two do not agree in the details, the reason probably being that the loop sets used in the two studies are not exactly the same. Interestingly, in his comparative analysis, Ford confirms that the loop *L3* is dominant but concludes that the loop *L5* is not. He does not consider other influential loops such as the overtime loop (the Production scheduling loop in this study) as mentioned in Kampmann. This phase corresponds to the phases II, III, and IV in Oliva and Mojtahedzadeh (2004) where they identify the Supply first-order control, the Capital expansion, and the Economic growth loops, respectively, as the most influential structures. Their most influential structures agree with the ones identified in this analysis. Nevertheless, different from the above analysis, they identify a single dominant structure at each phase, a characteristic of the PPM approach. Another difference is that the loops identified as the most influential structures in this study continue to be so throughout the second phase, which is chopped into three more phases each dominated by another loop in Oliva and Mojtahedzadeh (2004).

At the third, capital deceleration phase the net rate of increase in *Capital* slows down and even begins to decrease towards the end of the phase. At the start of the phase, the relatively stronger influences of Backlog expansion (*L6*) and Self-ordering (*L14*) loops can be distinguished. Then Self-ordering loop becomes the most influential one but looses its influence towards the end of the phase. In contrast, the influences of Supply first-order, Order fulfillment, Economic growth and Production scheduling loops show increase (Figure 18.d). This corresponds to the beginning of the decrease in the rate of increase in *Capital*. This phase is part of phase III in Kampmann. The two studies agree in that the self-ordering is the most influential on average over the whole interval but somewhat differs in the details. The same conclusion holds regarding the Ford's analysis. The capital deceleration phase coincides with the beginning of the phase V of Oliva and Mojtahedzadeh (2004). They identify the Supply first order control loop as the most influential during this phase.

The Production scheduling loop becomes dominant at the first half of the Capital peak-then-decline phase. During this phase, the drop in *Backlog* that began in the previous phase continues; this relaxes the capacity utilization and the Production scheduling loop becomes dominant. The loop exerts its influence by drawing *Capital* stock downward thus it first slows down; then the Supply first-order loop takes the place of the Production scheduling loop as the most dominant, stops the growth of the stock and then causes it to drop precipitously right after it peaks. Nevertheless, this fast decline does not last long because the dominance of the loop drops while that of capital decay loop increases enough to shift the behavior of *Capital* to exponential decay. This happens around year 157. This phase coincides with the second half of Kampmann's phase III and most of the phase V of Oliva and Mojtahedzadeh (2004).

It is worth to note that Sterman also reports that when the capacity utilization is at its maximum the Capital expansion (*L5*) is dominant. In time, as excess capacity develops, the capacity utilization drops and dominance shifts to the Production scheduling loop which limits the amplitude of the cycle (footnote 26 on p. 45 of Sterman 1985). This line of events corresponds to the second phase through the first half of the fourth phase of the EEA and except the third phase where the Self-ordering loop (L14) is dominant the two explanations agree. They differ, however, in the corresponding dominant eigenvalues as discussed in the next section.

The transition from the fourth phase to the fifth is not sharp. The loops exchange dominance gradually from approximately year 156 to 158. During this phase, most of the feedback loops are shut off by the nonlinearities in the system and *Capital* slowly falls under the influence of capital decay loop until the cycle repeats itself. The findings for this phase agree with those from the previous studies.

5. Discussion and Conclusion

In spite of the guiding principle of the system dynamics that the behavior is generated as a result of the interactions between various feedback mechanisms of the system, the accurate depiction of the relationship between a model's structure and its behavior still rests upon an experimental process of hypotheses testing by repeated simulations. This approach is time consuming and prone to error on the analyst's part. Therefore, System Dynamics has much to gain from development of formal methods for model analysis. The methodology proposed in this paper consists of ten steps and advances the application of the EEA in loop dominance identification. The improvements proposed in this paper are summarized in the following.

1. It is possible to relate the loop dominance dynamics directly to any selected state variable through its net rate (i.e. slope). One criticism directed to the EEA has been its inability to relate the loop dominance to a variable of interest. This improvement addresses this criticism.
2. An improved approach based on Oliva (2004) in identifying the independent loop set is incorporated into the model analysis. The improved approach almost always finds a unique set and hence the problem of arbitrary selection of the members of the set is alleviated.
3. A new loop dominance measure is proposed which takes all behavior modes of the model under study into account.
4. For the selected models, the loop elasticities are actually plotted over time thus allowing for the visualization of how loop dominance dynamics unfold over time.
5. Many parts of the proposed procedure are already codified. Tools for others are either available in commercial software packages or it is the author's opinion that they can be readily codified if sufficient interest develops.

In addition, three models selected from the previous loop dominance studies were used to demonstrate the implementation of the proposed methodology. This also facilitated the comparison of the proposed version of the EEA with other formal model analysis approaches giving an opportunity to identify the strengths and weaknesses of each approach. Such comparative studies should continue to be conducted in the future in order to refine the existing formal analysis tools.

Of the three analyses, the one on the long wave deserves a closer look. It is generally believed that complex eigenvalue pairs are responsible for the turning points in a cycle. In this respect, the EEA of the long wave model leads to a rather counterintuitive observation on the generation of the long wave cycle. For the minimum of the cycle the analysis confirms the mentioned belief: During the first phase, there is a complex conjugate pair of eigenvalues and the pair is responsible for the transition of the Capital from decay to exponential growth (see Figures 15-16).

The situation, however, is different for the maximum of the cycle. The Capital reaches its peak within Phase four where there are three distinct negative eigenvalues. In order to understand the formation of the peak we need to look at what happens earlier, i.e. in the phases two, three, and four. Figure 19 presents the eigenvalues together with the Capital and its rate (slope), respectively, through these three phases. In Phase two, there are three distinct real eigenvalues of which the largest positive one is the dominant (see Figures C.5-16). The result is the ever-increasing rate, which causes the Capital to increase faster and faster. Then two of the eigenvalues coalesce and form a complex conjugate pair of eigenvalues. The complex pair is almost solely responsible for the behavior of the Capital in this third phase (see Figures C.5-16). Their effect can be observed on the behavior of the rate of the Capital, the increase of which first slows down; then, reverses and the slope begins to decrease (Figure 19.a). This, of course, exhibits itself as an inflection point on the behavior of the Capital after which the increase in the Capital begins to slow down (Figure 19.b). The third phase is, then in a sense where the complex pair prepares via its rate the

downturn of the Capital, which is to happen in the next, fourth phase. At around year 152, another bifurcation occurs resulting in three distinct negative eigenvalues; hence the fourth phase. Now, under the influence of the negative eigenvalues the rate exhibits decay until about year 157 which also marks the transition from the fourth to the last phase of the cycle (Figure 19.a). The rate exhibits decay; however, as long as it is positive the Capital continues to grow albeit slower and slower (Figure 19.b). Towards year 154, the rate becomes negative continuing its decay. At that instant, the Capital reaches its peak and then begins to decrease. The behavior exhibited by the Capital until about year 157 is actually exponential decline because its rate becomes more and more negative. In the last phase, the rate no longer drops but this time exhibits decay in the opposite direction, i.e. towards zero. Consequently, the behavior of the Capital changes from exponential decline to exponential decay.

What the EEA analysis tells us about the peak in the Capital is that the system prepares itself for the peaking by entering and then leaving the oscillatory mode well in advance of the time the Capital peaks. Rather the complex eigenvalue pair, with some influence from the negative eigenvalue, causes the peak in its rate in the third phase. In the forth phase in which the peak in the Capital occurs, the system has already left the oscillatory mode and now is in fact in a goal-seeking mode, which is evidenced by the behavior of the rate of the Capital. However, the system is so charged during –to some extent- the second, -but mainly- third phases that the crossing of the rate from positive to negative during its decay in the forth phase causes the Capital to slow down its growth and then to decline, causing the peak in the Capital.

Although the loops identified being dominant in this study and that of Sterman's mostly agree the two differ is their findings regarding the dominant behavior modes (i.e., eigenvalues), especially in the second through forth phases of the cycle. According to the EEA, the dominant behavior modes for the first and third phases are divergent oscillations (i.e., complex conjugate eigenvalue pairs with real parts). These phases correspond to the beginning and end of the time interval during which the capacity utilization is at its maximum. The rest of this interval constitutes the second phase and the dominant behavior mode is monotonic divergent (There are three real distinct eigenvalues the most positive of which is the dominant). The second and third phases correspond to what Sterman termed "the expansion phase" for which he mentions only the divergent oscillatory behavior mode (i.e., a complex eigenvalue pair with real parts) as dominant. In the forth phase as capacity utilization drops, there are three monotonic convergent behavior modes (i.e., real and distinct negative eigenvalues). Therefore the dominant behavior mode during the peak of the Capital is not a damped oscillation as suggested in Sterman but a combination of exponential decay modes. In other words, the amplitude of the Capital is limited by monotonic convergent behavior modes, not by a highly damped oscillation.

One of the problems of the earlier EEA applications was the lack of an explicitly specified variable of interest in the analysis. Specifying a variable of interest makes the results of the analysis more rigorous and relevant. In a typical EEA study, only one behavior mode is regarded as dominant at each analysis time step. Hence, the resulting explanation on loop dominance would be based on that behavior mode. In this study all behavior modes are considered to the extend of their contribution to the behavior of the variable of interest at each time step and a conglomerate measure for loop dominance is devised based on this approach. Finally, the previous applications of the EEA fell short of providing results that show the continuous and gradual change in loop dominance dynamics over time. That gap is also closed in this study. The differences between the proposed methodology and the earlier applications of the EEA are demonstrated on the long wave model analysis.

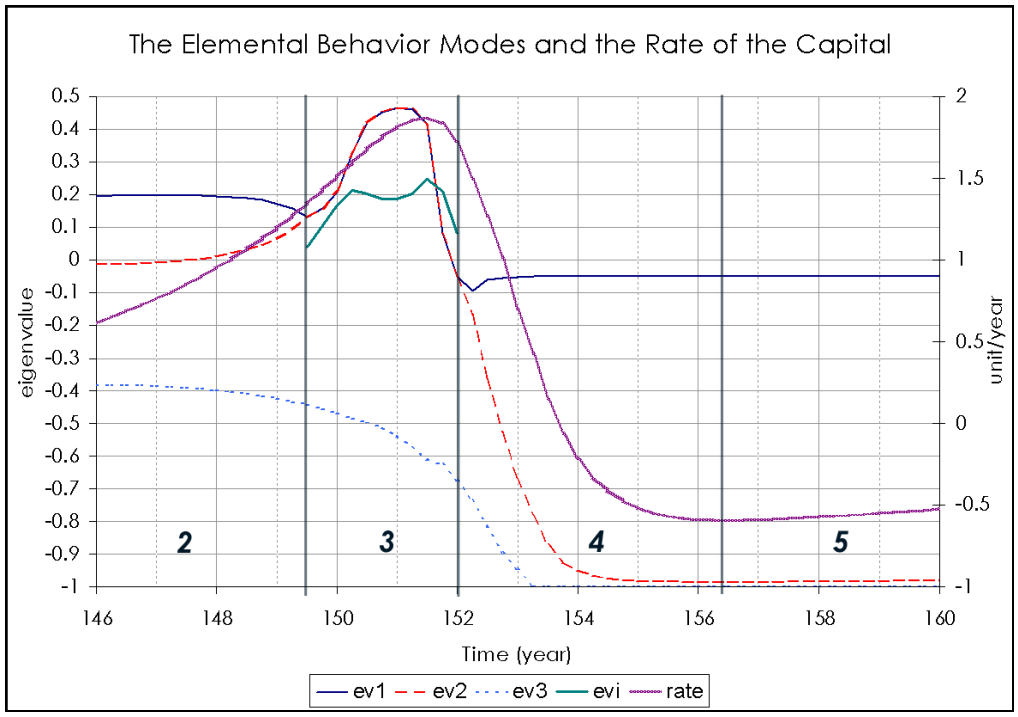

(a)

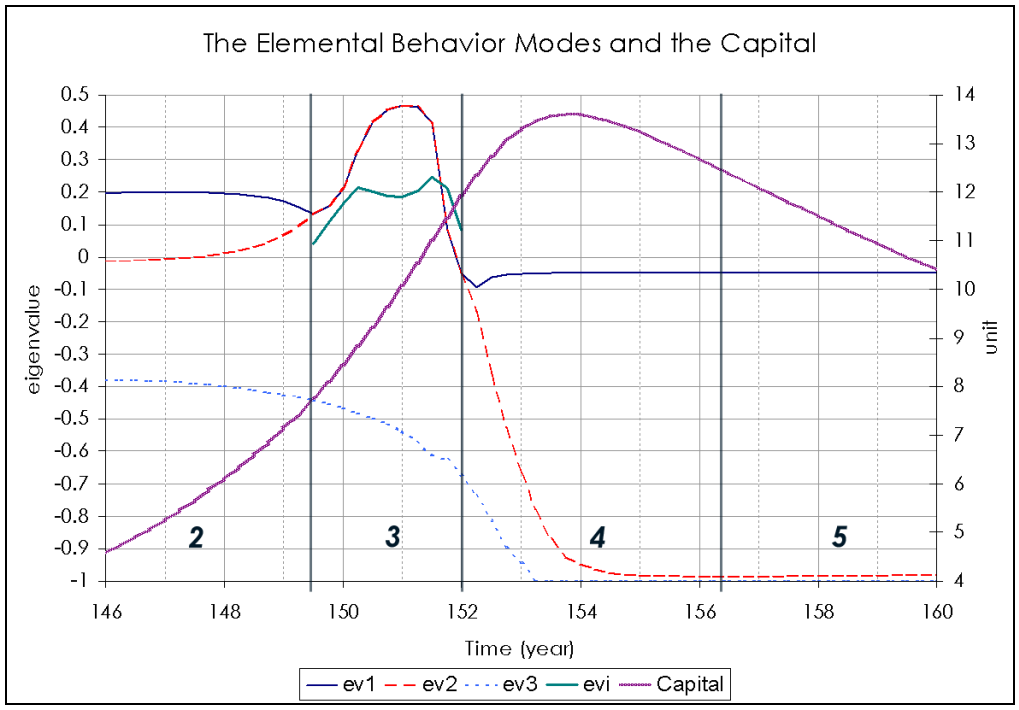

(b)

Figure 19. The behavior modes (eigenvalues), the rate of change in Capital *(a)* and Capital *(b)* in the third, fourth phases and parts of second and fifth phases.

There is a close relationship between the eigenvalues and the total participation metric in linear systems. Mojtahedzadeh *et al.* 2004 has shown that for any linear system regardless of the order of the system the total participation metric is equal to the largest eigenvalue of the system in the steady-state condition.

Still, the most important difference between the EEA and the PPM approaches is that the first approaches structure-behavior relations from a system-wide perspective while the latter adopts a localized perspective. The results one gets from the two methods may not always be in agreement because of the different perspectives the two approaches take on in loop dominance analysis. For instance, although in the Predator-Prey example the explanations from the two approaches are mostly in agreement it seems the PPM approach do not appropriately relate relevant parts of the model structure to the model behavior in case of oscillatory behavior. In another comparative study, a linear oscillatory model was used and there was even more disagreement between the results of the two approaches over the structural source of oscillations (results not shown). It may be the case that the level of agreement between the two is higher when they are applied to nonlinear models. It is, however, worth mentioning that the application of both EEA and PPM on a simple long wave model resulted in the same loops as the most influential ones in the generation of the cycle. Moreover, these loops are the ones selected by the loop selection algorithm (SILS) proposed by Oliva (2004). This suggests that it may be possible for other –more complicated– system dynamics models to reach an intuitive understanding of model dynamics (including the loop dominance dynamics) based on the loops selected in the SILS of those models.

Although there have been notable improvements in the EEA as a formal model analysis tool since it was first advocated more than twenty years ago, there is still need for further refinement of the methodology. For instance, the proposed overall loop dominance measure performed well in the examples but their real utility will show itself only after many applications on various system dynamics models. SILS approach is no doubt useful in loop dominance analysis but needs to be used with scrutiny and may require suitable revisions in the future. More importantly, there is still much to be done for fully computerized implementation of EEA routines. As an example, setting up equations for the causal link elasticities seems to be the routine that is most time-consuming. The successful automation of this step would greatly reduce the duration of analysis. In addition, most of the codes presented are either tailored for models of a specific order or for a specific model. While useful the set of codes presented in this study only serves as a starting point and more elaborate ones are required for the proper computerized implementation of EEA.

The work presented in this paper is part of a larger study. The next phase will focus on understanding how uncertainty in parameter values in a model affect its loop dominance dynamics and will look into devising ways to differentiate the contribution of each uncertainty source to the uncertainty of dominance dynamics by coupling the EEA approach with the error analysis.

Finally, it should be emphasized that existing approaches to loop dominance analysis may have much to learn from each other. As a result, it would not be surprising to witness the integration of best aspects of the different formal tools in the future.

References

Davidsen P. 1991. The structure-behavior graph. The System Dynamics Group, MIT, Cambridge.

Eberlein R. 1984. *Simplifying Dynamic Models by Retaining Selected Behavior Modes*. PhD Dissertation, MIT, Cambridge, MA.

Ford D. 1999. A behavioral approach to feedback loop dominance analysis. *System Dynamics Review* 15(1): 3-36.

Forrester N. 1982. *A Dynamic Synthesis of Basic Macroeconomic Theory: Implications for Stabilization Policy Analysis*. PhD Dissertation, MIT, Cambridge, MA.

—— . 1983. Eigenvalue analysis of dominant feedback loops. *The 1983 International System Dynamics Conference, Plenary Session Papers,* pp. 178-202. System Dynamics Society, Albany, NY.

Franklin GF, Powell JD, Emami-Naeini A. 2002. *Feedback Control of Dynamic Systems*. Fourth Edition. Prentice Hall Inc., NJ.

Gertner GZ. 1987. Approximating precision in simulation projections: An efficient alternative to Monte Carlo methods. *Forest Science* 33: 230-238.

Gonçalves P, Lertpattarapong C, Hines J. 2000. Implementing formal model analysis. *Proceedings of the 2000 International System Dynamics Conference*, *Bergen, Norway*. System Dynamics Society, Albany, NY.

Graham AK. 1977. *Principles of the Relationship Between Structure and Behavior of Dynamic Systems*. PhD Dissertation, MIT, Cambridge, MA.

Güneralp B. 2004. A principle on structure-behavior relations in system dynamics models. *Proceedings of the 2004 International System Dynamics Conference*, *Oxford, UK*. System Dynamics Society, Albany, NY.

Kampmann C. 1996. Feedback loop gains ans system behavior. *Proceedings of the 1996 International System Dynamics Conference*, *Boston, MA*. System Dynamics Society, Albany, NY.

Mojtahedzadeh MT. 1997. *A Path Taken: Computer Assisted Heuristics for Understanding Dynamic Systems*. PhD Dissertation, University at Albany, SUNY, Albany, NY.

Mojtahedzadeh MT, Andersen DF, Richardson GP. 2004. Using *Digest* to implement the pathway participation method for detecting influential system structure. *System Dynamics Review* 20(1): 1-20.

Oliva R. 2004. Model structure analysis through graph theory: partition heuristics and feedback structure decomposition. *System Dynamics Review* 20(4): 313-336.

Oliva R, Mojtahedzadeh MT. 2004. Keep it simple: dominance assessment of short feedback loops. *Proceedings of the 2004 International System Dynamics Conference*, *Oxford, UK*. System Dynamics Society, Albany, NY.

Richardson GP. 1995. Loop polarity, loop dominance, and the concept of dominant polarity. *System Dynamics Review* 11(1): 67-88.

—— . 1996. Problems for the future of system dynamics. *System Dynamics Review* 12(2): 141-157.

Saleh MM. 2002. *The Characterization of Model Behavior and its Causal Foundation*. PhD Dissertation, University of Bergen, Bergen, Norway.

Sterman JD. 1985. A behavioral model of the economic long wave. *Journal of Economic Behavior and Organization* 6: 17-53.